Wearable Second Harmonic Generation Imaging: The Sarcomeric Bridge to the Clinic

Justin C. Williams[1] and Paul J. Campagnola[1,*]
[1]Department of Biomedical Engineering, University of Wisconsin–Madison, 1550 Engineering Drive, Madison, WI 53706, USA
*Correspondence: pcampagnola@wisc.edu
http://dx.doi.org/10.1016/j.neuron.2015.12.009

Imaging of sarcomere dynamics in vivo in patients has significant clinical importance, as the structure and function is altered in numerous pathologies. In this issue of *Neuron*, Schnitzer and coworkers (Sanchez et al., 2015) demonstrate this capability through a miniature, wearable Second Harmonic Generation microscope.

Normal sarcomeric structure and contractile dynamics are disrupted in numerous disorders including cerebral palsy, myotonic dystrophy, amyotrophic lateral sclerosis, and sarcopenia as well as in damage occurring from stroke or other injury. Despite the clinical importance of imaging the individual motor units in such conditions, no high-resolution imaging technique has been available to image these dynamics in live animals or patients.

A crucial piece of determining function lies in measuring the sarcomere length, as this is the underlying contractile apparatus. Traditional ways of measuring sarcomere length and organization required tissue excision and then using electron microscopy, polarization microscopy, or histology. These methods require significant processing, and image thin single sections, and thus only provide a limited data set. More recently, the nonlinear optical microscopy technique of Second Harmonic Generation (SHG) has been implemented to interrogate sarcomeric structure in skeletal muscle tissues (Plotnikov et al., 2006). Similar to two-photon excited fluorescence (TPEF) microscopy, SHG imaging achieves intrinsic 3D imaging as single optical planes can be both excited and imaged. As near-infrared wavelengths are used (~700–1000 nm), penetrations depths of several hundred microns are often achievable. Critically, the contrast is endogenous, relying on the organization and birefringence of the tissue (Campagnola et al., 2002). As a consequence, the actual actomyosin assembly is imaged, rather than relying on inferences from exogenous fluorescent markers or fluorescent proteins. There has been significant work using SHG to understand the contrast mechanism from sarcomeres and also then use this information to probe structural changes. For example, it is now understood that contrast arises from the myosin heavy chain, with the dominant contributions arising from the tails rather than the heads (Plotnikov et al., 2006). The sarcomere lengths and distributions thereof can also be used to differentiate different muscle diseases states (e.g., mild and severe muscular dystrophy, atrophy, and aging with high specificity; Plotnikov et al., 2008). A limiting aspect of these studies is that the data acquisition was always performed from ex vivo tissues. However, this collective body of work suggests the power of performing SHG in vivo to assess sarcomeric structure in a variety of pathological conditions such as recovery from injury, from rehabilitation from stroke, or in degenerative diseases.

In this issue of *Neuron*, Schnitzer and coworkers (Sanchez et al., 2015) have integrated these previous concepts of SHG imaging to examine sarcomere organization in human patients in vivo. To this end, they constructed a miniaturized microscope that attached to the desired limb and was then coupled to the remainder of the electronics (control electronics, lasers, data acquisition). They acquired data on sarcomere length coupled with electrical stimulation from normal patients, from stroke patients on both affected and unaffected limbs, and from patients recovering from injury. This is a groundbreaking study that represents the first true in vivo imaging of muscle structure in human patients. Here we will describe the ground breaking instrumentation and also the contribution to neuroscience.

As SHG imaging has grown into an increasingly used high-resolution imaging modality, especially for probing diseased states (musculoskeletal, cancers, fibroses) (Campagnola, 2011), there has been concurrent interest in developing miniaturized and/or endoscopic approaches (Wu et al., 2009). These have taken a few different forms, depending on the targeted tissue type. Proximal scanning approaches typically use piezo scanners attached to the end of a single-mode optical fiber, where this scheme is appropriate for imaging open cavities such as the GI track. The other approach utilizes distal scanning, where the scanned light is coupled into a fiber, and the scanning electronics are remote. This idea has been previously used with miniaturized head-worn microscopes for mice using TPEF, where superficial regions of the brain were imaged through a cranial window (Helmchen et al., 2001). This has also been implemented with GRIN (gradient refractive index), or stick lenses or other fiber endoscope probes that penetrated the skin. The Schnitzer lab previously used this idea to minimally invasively image sarcomeres in mice and humans, although it still required a surgical procedure (Llewellyn et al., 2008).

The work here integrates many of these concepts into a wearable microscope. The picture of the device located on a human leg is shown in Figure 1A, and the schematic diagram is given in Figure 1B. In this device, light is coupled into the miniature microscope and scanned via a MEMS mirror, which is then relayed by a 0.65 mm diameter microlens assembly encased in a hypodermic needle. This punctures the tissue using a spring-loaded injector that moves the probe through the skin, fat, and fascia and into the muscle, where the location was image guided by

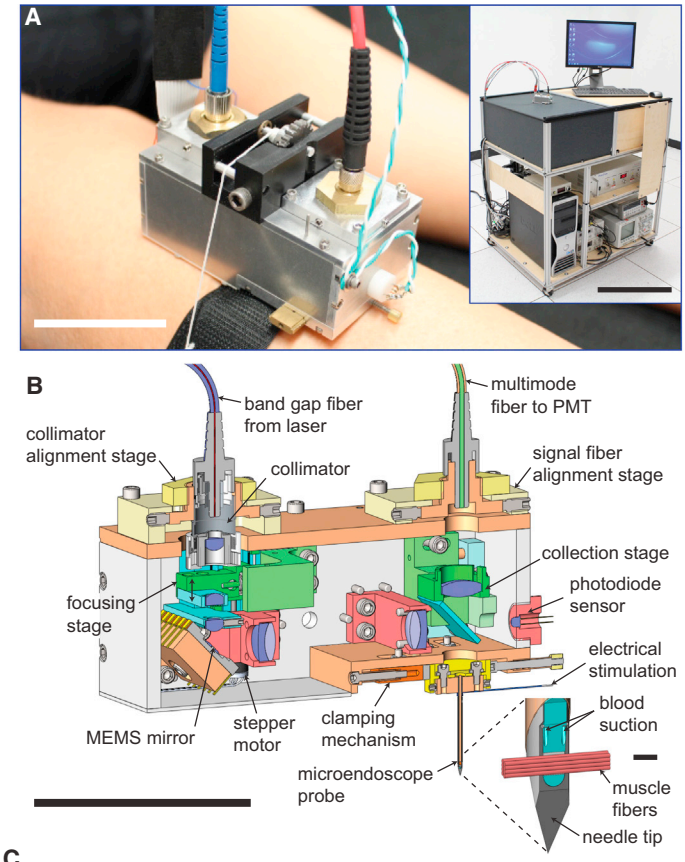

Figure 1. Description and Demonstration of Wearable SHG Microscope

(A) An alert subject wears the microscope during imaging of the tibialis anterior muscle. Two optical fibers that deliver laser illumination (blue sheath) and collect SHG signals (red sheath) provide flexible optical coupling to a mobile cart. (Inset) Light source, photodetector, and computer reside on the cart.

(B) Cross-section of the CAD diagram of the microscope, showing the housing, optical components, and electrical line used to excite motor neurons via the microendoscope. (Inset) Magnified view of the probe tip and the muscle fiber orientation during imaging.

(C and D) SHG line-scans of the biceps brachii of the relaxed, affected, and unaffected limb, respectively, of a poststroke subject. Scale bars are 10 μm (vertical) and 100 ms (horizontal).

Adapted from Sanchez et al. (2015).

ultrasound. A microprism is then attached to the end of the mini GRINS lens to afford right-angle viewing at a given depth into the muscle. A similar approach was used by Levene and coworkers for TPEF imaging at different levels of the mouse brain using an implanted prism (Andermann et al., 2013). A separate optical path collects the emitted SHG, which is fiber coupled to the remainder of the electronics located on a cart. The achievable field sizes were 78 × 78 μm and the resulting resolution was approximately 1.6 microns. These parameters are both sufficient for sampling numerous sarcomere lengths with sufficient resolution. Importantly, the flexibility of the two fiber optic cables (excitation and collection) permits patients to move comfortably when hooked up to the microscope. Additionally, the microlens assembly is encased in a needle that provides additional functionality, serving as a stimulating electrode for controlled activation of the surrounding muscle as well as providing multiple microfluidic fluid suction ports for clearing blood and other fluids to provide a clear imaging path between the lens and surrounding muscle.

The authors first validated the technology by imaging relaxed sarcomeres in alert human subjects in six locations from the arms and legs, where they determined the precision of sarcomere length measurements on single patients as well as the interpatient variability, where these were ~30 and 300 nm, respectively, and much less than the average sarcomere length (~3 μm). Additionally, the results were similar to previous ex vivo determinations of sarcomere lengths via SHG microscopy. They next coupled these measurements with stimulation through the electrode to view contraction in both alert humans and anesthetized mice, where the results conclusively showed the displacement was consistent with excitation of motor neurons, rather than direct stimulation of muscle action potentials. Further controls measuring contraction times showed the ability to stimulate both fast and slow motor units.

In the first measurement of its kind, the authors imaged sarcomeres in the biceps brachii muscles of patients with spasticity post hemiplegic strokes. Figures 1C and 1D show the resulting SHG line-scan images in the spastic and contralateral muscle, respectively. The former shows clear fasciculations and sustained contractions not present in the former. The sarcomere lengths were also different in the two biceps by about ~0.5 microns, where these differences were not present in approximately aged matched normal patients. As a comparison, the authors also imaged the sarcomere dynamics in patients with an injury to the biceps brachii muscle, and found sarcomere length differences in the damaged and normal arms; but unlike the stroke patients, no fasciculations or involuntary microscopic contractions were observed. The demonstrated ability

to perform such measurements in these disparate subject populations opens up the potential to use this technology to both diagnose and safely study a wide range of both diseased and even normal muscle conditions. Perhaps more important is the potential to study disease progression longitudinally, owing to the minimally invasive nature of the measurement.

The instrumentation permits probing sarcomere twitch dynamics in alert humans. The required data collection is approximately 15 min, and is completely reasonable, as it is comparable in length to procedures the same patient populations would undergo in standard clinical EMG muscle testing. Moreover, the procedures were well tolerated in the patients, allowing comparison with normal volunteers with poststroke or injured patients. A limiting aspect of the approach is the removal of the optical needle during posture changes, as the probe is rigid and impedes movement. Similarly, imaging during large muscle movements cannot be performed. These impediments could likely be overcome in future iterations. It is actually quite impressive that the current form, with all its capabilities, is the first published description of this technology, and it is only likely to lead to improvements in future iterations.

The technique permits the acquisition of never-before-possible dynamic information on sarcomere dynamics, where this has strong clinical applicability. For example, ex vivo studies of diseased and aged muscle tissues in both mice and humans have shown altered sarcomere lengths and alignments relative to normal tissue (Plotnikov et al., 2008). The instrumentation here could provide in vivo diagnostics, rather than relying on a painful, invasive biopsy. Additionally, this information could be valuable for surgical planning or other interventions for cerebral palsy or poststroke patients. With the ability to probe individual motor units, the technique could also replace the need for unpleasant needle EMG-based assessments. While the individual needles that are used for intramuscular EMG are typically much smaller than the optical probe shown in Figure 1B, they typically have to be inserted in multiple locations and depths within the muscle to obtain an accurate functional representation. In fact, it would be quite possible to integrate EMG recording within the optical probe assembly (Figure 1B). The stimulating electrode that was developed in the current study is quite elegantly used to house both the optical probe components as well as microfluidic ports for fluid suction. Given the fact that both the optical components and the fluidic components have microscale features, it is certainly conceivable that a microfabricated electrode (or even an array) could be incorporated into the optical probe for recording intramuscular EMG. It is even possible that electrodes could be incorporated into the optical interface itself, as recent reports on the use of optically transparent electrodes have enabled simultaneous imaging with electrical recording and stimulation from the same interface site (Park et al., 2014).

While the work here was directed at imaging muscle dynamics, SHG also has exquisite sensitivity to collagen organization (Chen et al., 2012). Thus, the worn SHG microscope could be altered to dynamically image the connective tissues in joints and tendons. For example, numerous tendon injuries and subsequent repair (and scarring) processes result in collagen structural changes that could be detected by SHG. While a penetrating needle probe may not be the most appropriate method for diagnosing those conditions, alternative designs that incorporate en face imaging of a tendon surface through a needle insertion may be equally valuable.

In vivo imaging has opened up a whole wealth of new information about disease processes, but so far dynamic studies have been limited mostly to animals due to the predominant use of extrinsically applied or constitutively expressed fluorescent labels in genetically modified animals. In particular, in vivo imaging methods have gained popularity in the nervous system, as the timescales of many physiological changes are relatively short. Additionally, a number of relevant neurological functions can be assessed with label-free imaging, including injury scarring (Schendel et al., 2014), metabolic activity and blood flow (Richner et al., 2015), and indirect measures of neural activity (Llano et al., 2009). The approach described here could also be employed in a number of different clinical disease diagnosis and treatment paradigms, especially where neural tissue is already exposed during another surgical procedure, or where implantable devices are inserted for short periods of time for longitudinal monitoring (Felton et al., 2007).

In vivo imaging of diseases and other pathological conditions in humans has been the long-term dream of SHG microscopy, as it has substantial power in imaging tissue alterations with endogenous contrast. The patient-worn miniaturized SHG microscope developed and demonstrated by Schnitzer and coworkers is a large step in that direction. The technology will have great clinical applicability, due to its sensitivity, specificity, resolution, and appropriate footprint.

REFERENCES

Andermann, M.L., Gilfoy, N.B., Goldey, G.J., Sachdev, R.N., Wölfel, M., McCormick, D.A., Reid, R.C., and Levene, M.J. (2013). Neuron *80*, 900–913.

Campagnola, P. (2011). Anal. Chem. *83*, 3224–3231.

Campagnola, P.J., Millard, A.C., Terasaki, M., Hoppe, P.E., Malone, C.J., and Mohler, W.A. (2002). Biophys. J. *82*, 493–508.

Chen, X., Nadiarynkh, O., Plotnikov, S., and Campagnola, P.J. (2012). Nat. Protoc. *7*, 654–669.

Felton, E.A., Wilson, J.A., Williams, J.C., and Garell, P.C. (2007). J. Neurosurg. *106*, 495–500.

Helmchen, F., Fee, M.S., Tank, D.W., and Denk, W. (2001). Neuron *31*, 903–912.

Llano, D.A., Theyel, B.B., Mallik, A.K., Sherman, S.M., and Issa, N.P. (2009). J. Neurophysiol. *101*, 3325–3340.

Llewellyn, M.E., Barretto, R.P., Delp, S.L., and Schnitzer, M.J. (2008). Nature *454*, 784–788.

Park, D.W., Schendel, A.A., Mikael, S., Brodnick, S.K., Richner, T.J., Ness, J.P., Hayat, M.R., Atry, F., Frye, S.T., Pashaie, R., et al. (2014). Nat. Commun. *5*, 5258.

Plotnikov, S.V., Millard, A.C., Campagnola, P.J., and Mohler, W.A. (2006). Biophys. J. *90*, 693–703.

Plotnikov, S.V., Kenny, A.M., Walsh, S.J., Zubrowski, B., Joseph, C., Scranton, V.L., Kuchel, G.A., Dauser, D., Xu, M., Pilbeam, C.C., et al. (2008). J. Biomed. Opt. *13*, 044018.

Richner, T.J., Baumgartner, R., Brodnick, S.K., Azimipour, M., Krugner-Higby, L.A., Eliceiri, K.W., Williams, J.C., and Pashaie, R. (2015). J. Cereb. Blood Flow Metab. *35*, 140–147.

Sanchez, G.N., Sinha, S., Liske, H., Chen, X., Nguyen, V., Delp, S.L., and Schnitzer, M.J. (2015). Neuron *88*, this issue, 1109–1120.

Schendel, A.A., Nonte, M.W., Vokoun, C., Richner, T.J., Brodnick, S.K., Atry, F., Frye, S., Bostrom, P., Pashaie, R., Thongpang, S., et al. (2014). J. Neural Eng. *11*, 046011.

Wu, Y., Leng, Y., Xi, J., and Li, X. (2009). Opt. Express *17*, 7907–7915.